CRYSTALLIZATION FOULING IN DOMESTIC APPLIANCES AND SYSTEMS

Amthal Al-Gailani*, Thibaut Charpentier, Olujide Sanni and Anne Neville

Institute of Functional Surfaces, School of Mechanical Engineering, University of Leeds,

Leeds, LS2 9JT, United Kingdom

Abstract

The complex problem of inorganic scale formation on heat transfer surfaces is of substantial importance for industrial and domestic systems. Formation of mineral scale, particularly calcium carbonate, has long been a concern in domestic appliances such as boilers, steamers and washing machines. Here, the formation of solid inorganic deposits was studied on solid surfaces and in the bulk solution as a result of evaporation of natural potable water. Scale precipitation rates were evaluated for metallic samples for various bulk temperatures, surface roughness values and as a function of time. The morphology of crystals from both surface and solution was evaluated. The concentration of calcium ions was evaluated using Atomic Absorption Spectrophotometry (AAS), in order to investigate the kinetics of the precipitation reaction. The microstructure and morphology of deposits on the surface were analysed using Scanning Electron Microscopy (SEM) and X-ray diffraction (XRD). The present work has demonstrated that fouling deposition rates increase as the evaporation process proceeds as expected. The nature of the material and the surface roughness both affect surface deposition kinetics. The complex relationship between the saturation ratio (as the bulk solution shows precipitation) and the kinetics of bulk and surface precipitation/deposition is demonstrated. The prevailing crystalline form of calcium carbonate as detected by SEM and XRD is aragonite. However, the polymorphic composition of surface deposition and the bulk precipitate is influenced by temperature.

Keywords: Calcium carbonate, domestic systems, precipitation, temperature, roughness, tap water.

1. INTRODUCTION

Scale is often defined as the unwanted deposition of minerals on a heat transfer surface. It is an extremely common and complex problem in industrial and domestic systems where mineral water is a working fluid [1, 2]. The precipitated layer of inorganic salt generally comprises calcium carbonate, calcium sulphate, magnesium hydroxide, etc., generated by chemical reaction of cations and anions in a solution. An increase of the solution temperature promotes the reaction kinetics, nucleation and growth rate of crystal of a sparingly soluble inorganic scale [3, 4]. The resistance to heat transfer caused by scale fouling costs money by diminishing the efficiency of heat transfer. It also boosts the pressure fluctuations in systems by reducing the flow area, and increases maintenance cost and replacement works [5-9].

Fouling of heat transfer surfaces in domestic appliances results in environmental and economic impacts. The power consumption of electrical boilers, steam irons, washing machines, dishwashers and coffee makers is significantly increasing due to the low thermal conductivity of scale layer [10]. It is estimated that the heat transfer efficiency of gas water-boilers will be reduced by 30% over a period of 15 years if no effective mitigation strategy is applied [11]. Dobersek *et al.* [12] investigated the influence of the precipitated water scale on the consumption of electrical energy for domestic appliances. They found that scale layers of 2 mm thickness reduced the heat flow by 10% to 40%, depending on the composition of scale. For the same scale thickness, the power consumption of an electric boiler is two times higher than that for washing machine.

Temperature is one of the decisive crystallization parameters which can influence both saturation degree, reaction kinetics, and scale morphology. In the work of Yang *et al.* [13], the effect of surface temperature on scale formation on the copper-modified surface has been examined. The temperature increase from 70.8 ℃ to 82.8 ℃ resulted in fouling resistance increase by more than 7 times. The presence of mineral ions in water may pose an impact on the growth process of scale crystals. Chen *et al.* [14] reported that the kinetics of $CaCO_3$ bulk precipitation for different concentrations of magnesium ions using rotating disk crystalliser (RDC). The results showed that Mg^{2+} has an inhibitory effect on the bulk precipitation as well as $CaCO_3$ polymorphic phases.

The surface roughness was shown to exert a remarkable impact on the tenacity of the calcium carbonate deposits. Keysar *et al.* [15] pointed out the shear stress for detaching the calcite crystals binding to the rough surface (R_a= 18-24 μm) was estimated to be as much as 30 times greater than that for smoother surface (R_a=0.1-0.15 μm). The results also revealed that the scale formed on the smooth surface was three times higher in porosity than that on the rougher one.

The pipe material is one of the quality criteria in a domestic appliance that represents heat transfer efficiency. The commonly used metals for this purpose are stainless steel, copper and aluminium. Substrate parameters such as surface energy and thermal conductivity could influence the scaling tendency, adhesion and morphology of scale [16-18]. Teng *et al.* [17] studied surface deposition rate on copper, aluminium, stainless steel, brass, and carbon steel. The highest amount of scale was deposited on copper while the lowest amount was deposited on stainless steel.

Investigations into crystallization fouling have largely focused on the surface deposition in the industrial systems using solutions saturated with calcium only and carbonate ions. The supersaturation of similar solutions at constant temperature decreases with time due to consumption of ions in the crystallization reaction. The water heating in the domestic devices mostly includes water evaporation. Aspects of the mechanism of the scaling process from tap water in domestic appliances under evaporation conditions are still not fully understood. Evaporation of test solution, besides Ca^{2+} and CO_3^{2-} consumption affect solution supersaturation. In the present study, the scale formation from potable water has been investigated in order to improve the understanding of fouling

mechanisms in domestic systems. The effects of solution temperature, surface roughness and surface material on the scale amount and morphology have been examined.

2. MATERIALS AND METHODS
2.1. Experimental set-up

Experiments are performed in a unique setup mimicking a batch evaporation system. The schematic drawing of the setup is presented in figure 1. It consists of a borosilicate glass beaker, hot plate, thermocouple, sample holder, and identical metallic samples. The sample holder is constructed of stainless steel for minimizing the potential of corrosion products formation. The temperature probe (Thermo Scientific, 88880150) was connected to the lab hot plate to control temperature in a 1000 ml borosilicate glass vessel. Eight cylindrical samples of each copper, aluminium, and stainless steel have been made with similar height and diameter of 10 ± 0.05 mm. The samples are fabricated with hollowed bottom with a depth of 8 ± 0.05 mm to be established on the sample's holder vertical fines. The top surfaces of all samples were initially polished by mechanical method to obtain surface roughness (R_a) of 8-24.6 nm.

Using the artificial hardened solutions for studying the scaling process may not provide a full understanding of fouling mechanisms in domestic systems. The presence of different ionic species in potable water may affect the fouling rate and scale morphology. The commercially available *Evian* bottled water has consequently been used as scaling test fluid. As *Evian* being a very hard water with hardness of 307 ppm of $CaCO_3$, it has been chosen for the test rather than tap water to accelerate scale formation. The diversity of ionic species in drinking or tap water may pose some influences on the fouling phenomenon. The composition of *Evian* water is listed in Table 1. Stainless steel samples with mirror-like surface have been used in the experiments to evaluate the temperature effect. The tested temperatures are 85, 95, and 105 ℃. The power consumed by the hot plane is ranging from 1748 to 2139 W. The rate of evaporation of water increases with water temperature due to increase in the kinetic energy of molecules (Fig. 2). In investigations of substrate effect, the three metallic surfaces; copper, aluminium, and stainless steel have been tested at constant roughness and bulk temperature of 95 ℃. Stainless steel samples subsequently used in the roughness experiments at a fixed bulk temperature of 95 ℃. Roughness average (R_a) is the roughness parameter that is adopted in the current work. The tested surface roughness values

are 10, 106, and 182 nm. To check the reproducibility of all experiments, the runs are repeated at least twice.

2.2. Surface and solution characterization

The top surfaces of all samples were mechanically polished to obtain a clean surface and particular surface roughness. Surface roughness parameters were evaluated prior to the experiments using the 3D optical profiler NPFlex (Bruker, USA). For every 100 ml of the evaporated water, a sample and 1 ml of solution were taken from the test vessel. The solution volume was mixed with 9 ml of a quenching (KCl/polyvinyl sulfonate) solution[1] to prevent further precipitation. The analysis of Ca^{2+} concentration of the resultant solution was carried out using the Atomic Absorption Spectrophotometry (AAS). The measured concentration of Ca^{2+} at different evaporated volumes was introduced to calculations of saturation ratio. The samples were dried at 37 °C for 24 hours, followed by scale mass measurement by a high accuracy lab balance. The deposit morphology was examined using a Philips X'Pert X-ray diffractometer and Carl Zeiss EVO MA15 SEM-EDX.

Table 1. Evian drinking water composition.

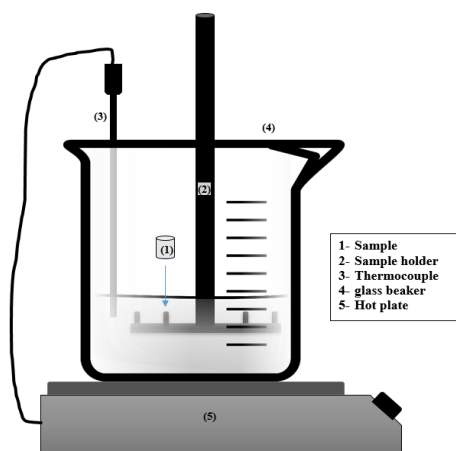| Ion	ppm
Ca^{2+}	80
Mg^{2+}	26
Na^+	6.5
K^+	1
Si^{4+}	15
HCO^{3-}	360
SO_4^{2-}	14
Cl^-	10
NO^{3-}	3.8
Dry residue at 180°C	345

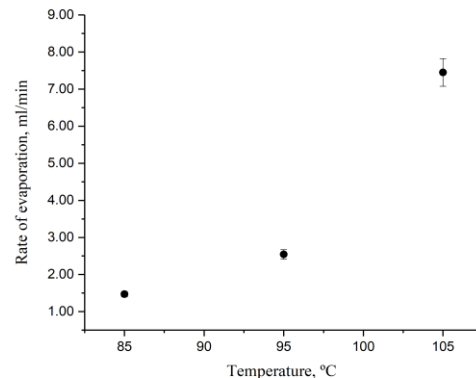*Figure 1. Schematic of the test set-up.*

Figure 2. The evaporation rate of solution at different temperatures.

3. RESULTS AND DISCUSSION

3.1. The effect of temperature

Fig. 3 shows the amount of scale precipitated on the stainless steel surface increases with the evaporated water volume and the bulk temperature. These findings was plotted based on the repeated experiments. Temperature increase from 30 to 90 °C reduces the solubility of $CaCO_3$ from 220 to 40 ppm, and hence increases the supersaturation and scaling tendency at a constant concentration of foulant [19]. The consumption of calcium ions in water by the crystallization reaction increases with the volume of evaporated water (Fig. 4). It can be seen from the exponential decay of calcium ions, the consumption rate of calcium in the solution is faster than the water evaporation rate, as such saturation ratio decreases with time, as reported in Fig. 3. The SEM observations in Fig. 5 show that the needle-like aragonite crystals are the dominant form of $CaCO_3$ at all tested temperatures with various amounts of mucus-like amorphous particles. The elemental analysis by Energy Dispersive X-Ray Analyser (EDX) shows that magnesium content in the amorphous particulate is slightly higher than that in aragonite particles (Spectrums 6 and 7 in Fig. 6). However, the magnesium may have an inhibitory effect on the morphological transformation to crystalline particles [20-22].

The XRD analysis of scale deposited on the surface illustrates that the aragonite is the prevailing polymorph $CaCO_3$ for all temperatures (Fig. 7). The solution temperature promotes the morphological transformation on the surface from vaterite and calcite to aragonite. In the XRD for precipitates in the bulk, a few changes have been spotted; namely, transformation of aragonite to calcite, and the

---

[1]Quenching solution was prepare by adding 1 mg of polyvinyl sulfonate (PVS) scale inhibitor and 5.71 gm of KCl in 1000 ml of distilled water.

3

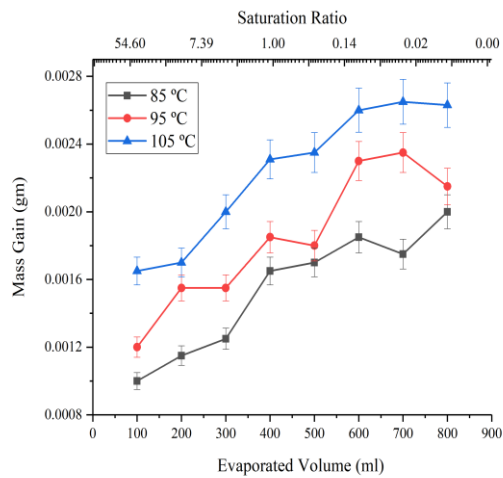presence of calcium sulfate (Anhydrite) in temperatures of 95 and 105 ºC (Fig. 8).

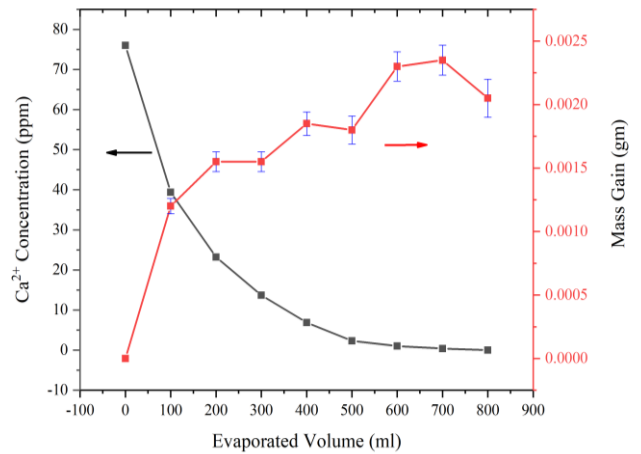Figure 3. Effect of temperature on the scale formation on stainless steel.

Figure 4. Effect of water evaporation on the Ca^{2+} concentration.

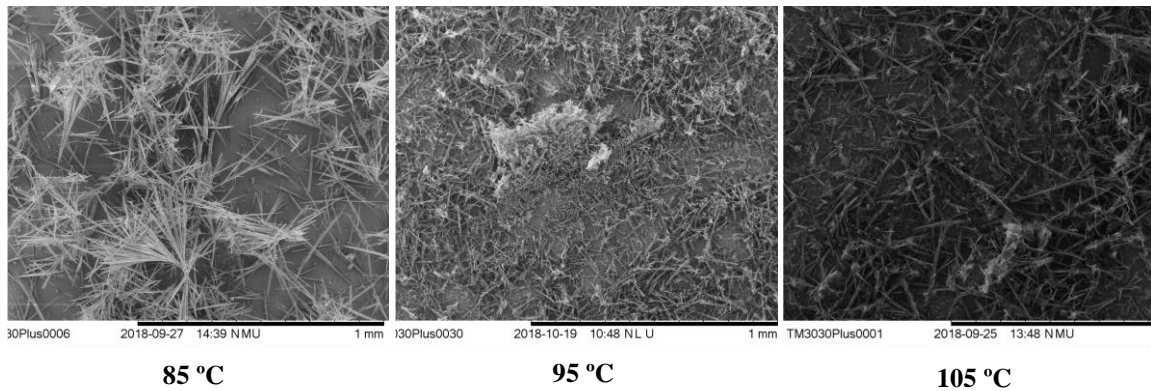**85 ºC**   **95 ºC**   **105 ºC**

Figure 5. SEM observations of scale crystals for a different solution temperature.
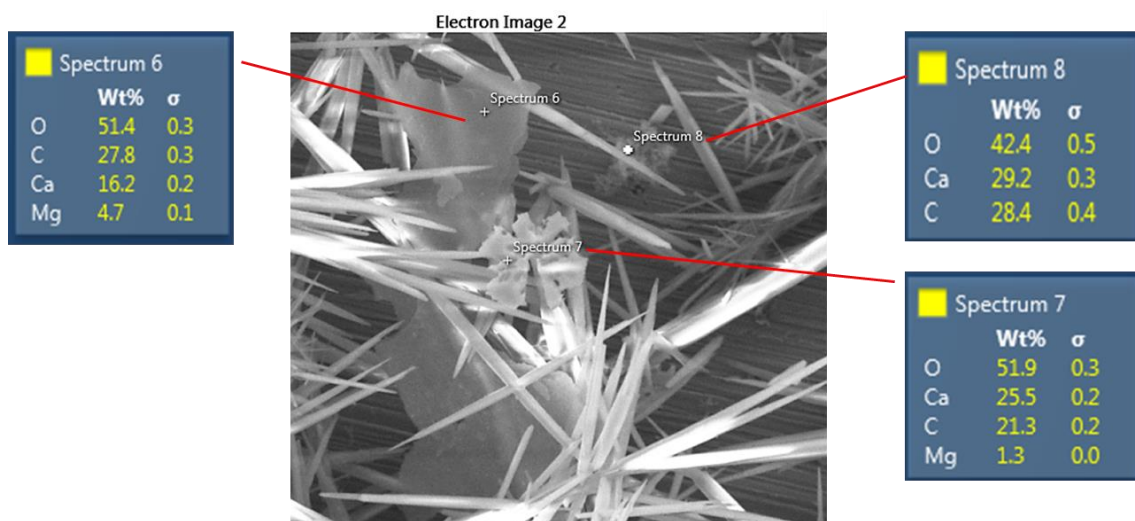

Figure 6. EDX elemental analysis for different forms of calcium carbonate deposits.
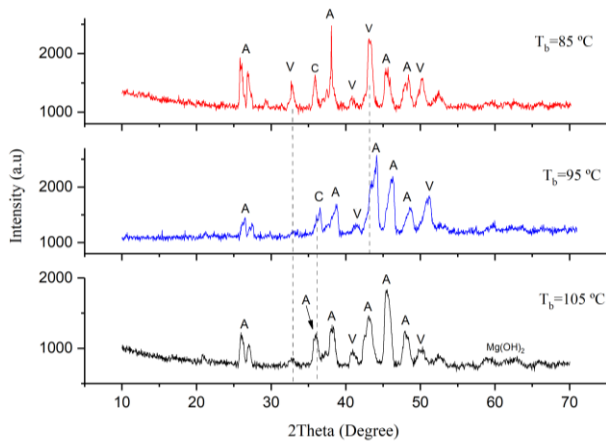
4

Figure 7. XRD analysis of the scale crystalline species on the surface (A: Aragonite, C: Calcite, and V: Vaterite).
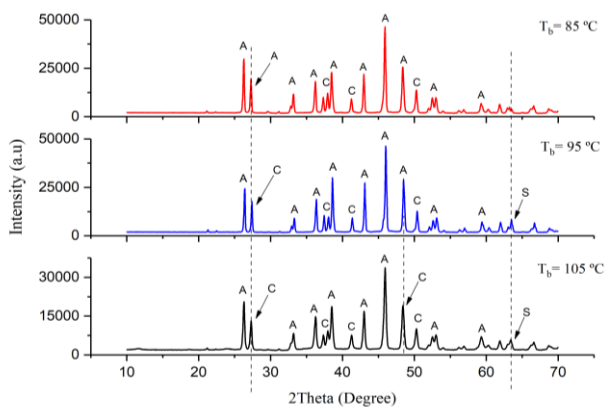

Figure 8. XRD observation of the bulk precipitation (S: calcium sulfate as anhydrite).

3.2. The effect of surface substrate

The visual observations showed that the aluminium sample was coated by a black layer. According to the SEM-EDX analysis, this porous black crust comprises of Al and O, and this strongly suggests it is an aluminium oxide (Al_2O_3) deposit (Fig. 9). No significant variation in the amount of the precipitated scale among the tested surfaces has been observed (Fig. 10). The mass gain on Al is a mixture of oxide layer and mineral deposits. As crystal forms in the bulk solution by the homogeneous nucleation, the surface may not affect the nucleation and growth process. The surface nature nevertheless can influence the adhesion properties with the precipitated crystal [23].

The common denominator among the deposits morphology on the different surfaces is the presence of non-crystalline species (Fig. 11). The amorphous particles on copper occupy larger area

compared with the other metals. The copper ions yielded as a corrosion product may inhibit the transformation from amorphous to crystalline form [24]. Al^{3+} ions also may behave similarly on aluminium substrate but with lower inhibitory efficiency as a consequence of the consumption of the ions in the oxidation reaction. It seems furthermore that the population of scale crystals on aluminium is relatively low and the oxide layer may provide a weaker adhesive strength per unit area. Regarding the scale structure on stainless steel, the secondary growth of the amorphous particulates might heterogeneously commence after the aragonite binding on the surface.

The XRD analysis shows differentiated findings in terms of the crystalline phase's abundance, crystal geometry, and the analysis intensity (Fig. 12). The $CaCO_3$ vaterite on copper is higher than that on the other materials. The higher amorphous particles on the surface the larger amount of vaterite crystals. The absence of ionic inhibitors (such as Al^{3+} and Cu^+) allows the transformation to aragonite form. Crystals of γ-alumina (γ-Al_2O_3) have been detected on aluminium, which confirms that the dark porous crust underneath the deposits is built of aluminium oxide.
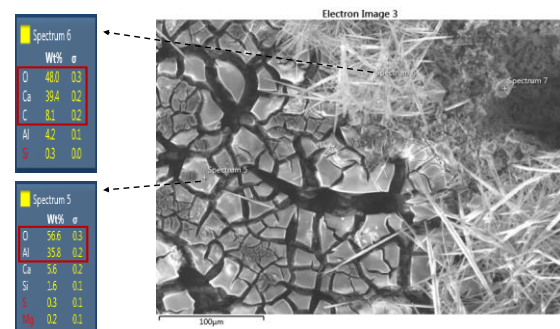

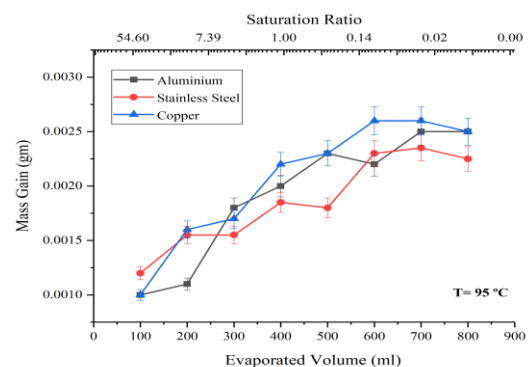*Figure 9. The EDX analysis for the oxide layer and scale crystals.*

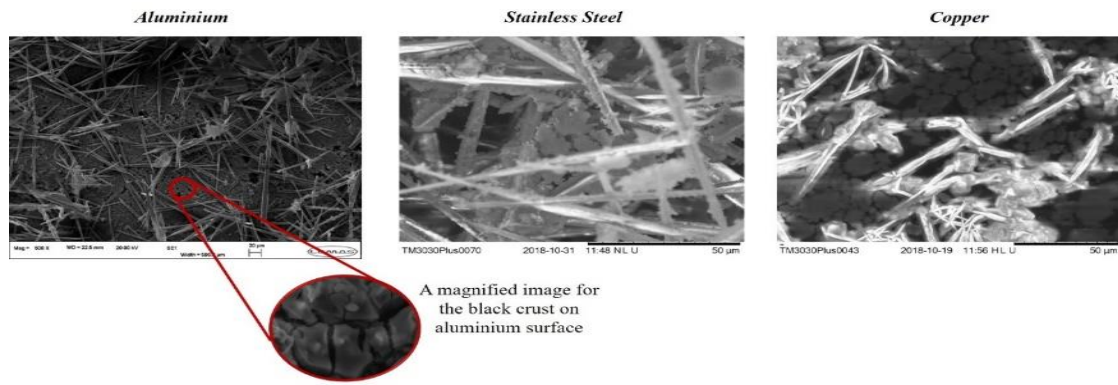Figure 10. Effect of surface substrate on the scale mass.

5

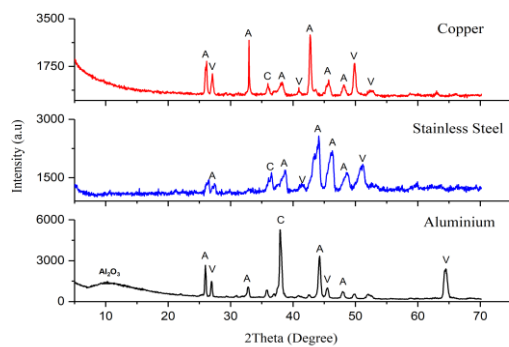*Figure 11. SEM images of scale crystals on a different substrate.*

Figure 12. XRD analysis of the scale crystalline species on different metals

3.3. The effect of surface roughness

Fig. 13 shows that the precipitated mass on all surfaces is very similar, particularly in the earlier stages of the evaporation. It seems that it is hard to remove the scale particles on the rougher surface by turbulent bubble circulation at the later stages of evaporation, where the water level is low. As the crystals are formed by homogenous crystallization, the influence of roughness concentrates on the aspects of particle-surface adhesion. The SEM observations in Fig. 14 show that the amount of deposit flakes increases with the roughness. It also illustrates that the flowers of aragonite formed

underneath the amorphous coat. However, the presence of these flakes can affect the accuracy of the XRD analysis. Many differences can be observed in the XRD measurements related to peaks intensity and position, and the detected polymorphs (Fig. 15). The significant morphological transformation paths include from calcite on the smooth surface to aragonite on the moderately rough surface. Then, the aragonite crystal on the surface with moderate roughness (R_a= 106 nm) transforms sequentially to vaterite particle on the rougher surface (R_a= 182 nm).
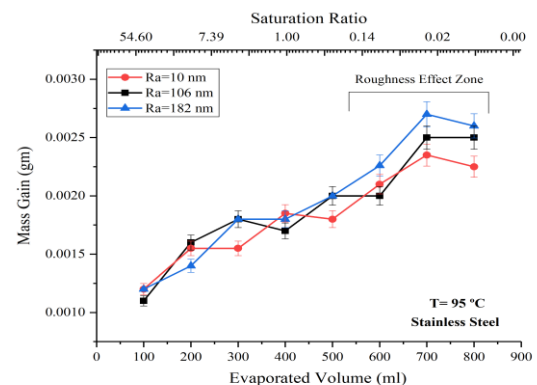

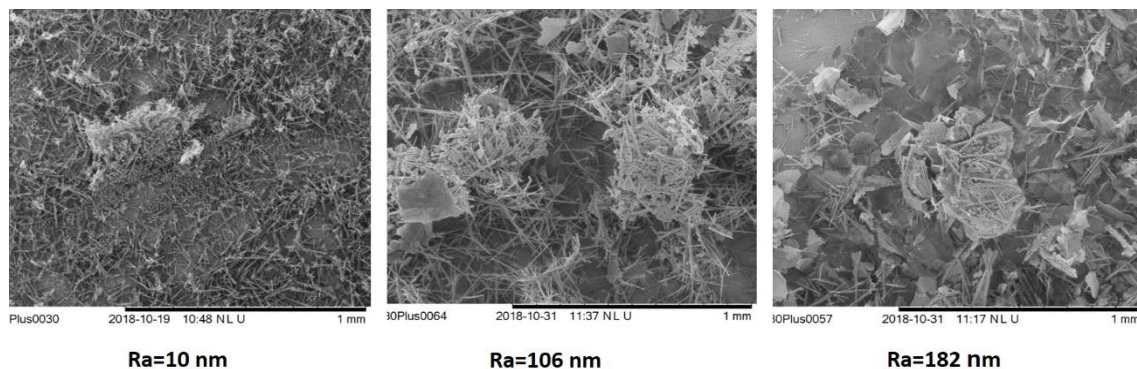
Figure 13. Effect of surface roughness on the scale mass.

Ra=10 nm   **Ra=106 nm**   **Ra=182 nm**

Figure 14. SEM images of scale deposits on surfaces with different roughness.
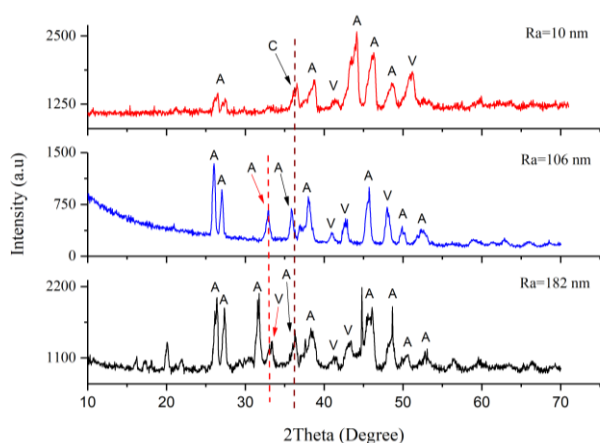
6

Figure 15. XRD analysis of the scale crystalline species on different roughness surfaces

4. CONCLUSIONS

Evaporation of mineral water in domestic appliances has generally been associated with precipitation of deposits from the bulk solution that binds onto appliance hot surfaces. The present work investigates the crystallization fouling with water evaporation process at different solution temperature, surface material, and surface roughness. The deposit mass predominantly increases with the volume of evaporated water, while Ca^{2+} solution content simultaneously decreases according to an exponential decay relationship. The solution temperature promotes the bulk precipitation and the polymorphic transformation from both calcite and vaterite to aragonite. It is found that flakes of amorphous species are formed above the crystalline particles.

The drinking water used in the experiments contains a variety of ions that contribute to crystal growth and scale morphology. The amount of amorphous particles increases with temperature and it consists of about 4% by weight of magnesium. Hence, this may explain how these non-crystalline particles are formed at a solution temperature of 95 ^{o}C. At the high temperatures, Mg^{2+} in water may interact with growing crystals and inhibits a further growth, leading to amorphous $CaCO_3$ formation rather than one of the polymorphic phases. Similarly, the scale structure on aluminium and copper surfaces is affected by the presence of Cu^+ and Al^{3+} which released as a corrosion products.

The effects of surface substrate and roughness were found be secondary on the precipitated mass under an evaporation effect. As the crystal forms in

the bulk solution by the homogeneous nucleation, a surface may not control the nucleation and growth process. The surface nature nevertheless can affect the adhesion force with the precipitated crystal. Particularly at the final stages of evaporation, the big precipitated crystals strongly attaches to a larger area of surface. The morphology analysis showed that calcite on the smooth surface turns into aragonite on surface with moderate roughness, and aragonite to vaterite on the rough surface. The results obtained in the present work may change if the water chemistry changed. A study of water quality influence is needed to draw complete representation of scaling in household appliances.

Abbreviations

A	*Aragonite*
AAS	*Atomic Absorption Spectrophotometry*
ACC	*Amorphous Calcium Carbonate*
C	*Calcite*
EDX	*Energy Dispersive X-Ray*
R_a	*Average Roughness*
S	*Calcium Sulfate Anhydrite*
SEM	*Scanning Electron Microscope*
V	*Vaterite*
XRD	*X-Ray Diffraction*

References

1. Chen, T., A. Neville, and M. Yuan, *Calcium carbonate scale formation—assessing the initial stages of precipitation and deposition.* Journal of Petroleum Science and Engineering, 2005. **46**(3): p. 185-194.
2. Steinhagen, R., H. Müller-Steinhagen, and K. Maani, *Problems and costs due to heat exchanger fouling in New Zealand industries.* Heat transfer engineering, 1993. **14**(1): p. 19-30.
3. Bott, T.R., *Fouling of heat exchangers.* 1995: Elsevier: p. 45-93 (1).
4. Epstein, N. *Fouling in heat exchangers.* in *Sixth International Heat Transfer Conference.* 1977.
5. DOBEROEK, D., D. Goricanec, and J. Krope, *The Influence of Physico-chemical Parameters on Water Scale Precipitation on Washing Machines' Heaters.* Acta chimica slovenica, 2007. **54**(4): p. 719-724.

7

6.   Krappe, J.M., *Scale Formation in Water Heaters and Methods of Prevention*. 1940: Purdue University: p. 27-40.

7.   Richards, C.S., F. Wang, W.C. Becker, and M.A. Edwards, *A 21st-Century Perspective on Calcium Carbonate Formation in Potable Water Systems*. Environmental Engineering Science, 2018. **35**(3): p. 143-158.

8.   Keogh, W., A. Neville, M. Huggan, V. Eroini, J.H. Olsen, F.M. Nielsen, S. Baraka-Lokmane, E. Bourdelet, J.A. Ellingsen, O. Bache, and T. Charpentier, *Deposition of Inorganic Carbonate, Sulfate, and Sulfide Scales on Antifouling Surfaces in Multiphase Flow*. Energy & Fuels, 2017. **31**(11): p. 11838-11851.

9.   Bukuaghangin, O., O. Sanni, N. Kapur, M. Huggan, A. Neville, and T. Charpentier, *Kinetics study of barium sulphate surface scaling and inhibition with a once-through flow system*. Journal of Petroleum Science and Engineering, 2016. **147**: p. 699-706.

10.   Brazeau, R.H., and M.A. Edwards, *A review of the sustainability of residential hot water infrastructure: Public health, environmental impacts, and consumer drivers*. College Publishing, 2011. **6**(4): p. 77-95.

11.   WQRF, *Softened Water Benefits Study: Energy Savings and Detergent Savings*. Water Quality Research Foundation, 2010.

12.   Dobersek, D., and D. Goricanec, *Influence of water scale on thermal flow losses of domestic appliances*. International journal of mathematical models and methods in applied sciences, 2007. **1**(2): p. 55-61.

13.   Yang, Q., J. Ding, and Z. Shen, *Investigation on fouling behaviors of low-energy surface and fouling fractal characteristics*. Chemical engineering science, 2000. **55**(4): p. 797-805.

14.   Chen, T., A. Neville, and M. Yuan, *Assessing the effect of Mg2+ on CaCO3 scale formation–bulk precipitation and surface deposition*. Journal of Crystal Growth, 2005. **275**(1-2): p. e1341-e1347.

15.   Keysar, S., R. Semiat, D. Hasson, and J. Yahalom, *Effect of surface roughness on the morphology of calcite crystallizing on mild steel*. Journal of colloid and interface science, 1994. **162**(2): p. 311-319.

16.   Zhao, Q., and X. Wang, *Heat transfer surfaces coated with fluorinated diamond-like carbon films to minimize scale formation*. Surface and Coatings Technology, 2005. **192**(1): p. 77-80.

17.   Teng, K., S. Kazi, A. Amiri, A. Habali, M. Bakar, B. Chew, A. Al-Shamma'a, A. Shaw, K. Solangi, and G. Khan, *Calcium carbonate fouling on double-pipe heat exchanger with different heat exchanging surfaces*. Powder Technology, 2017. **315**: p. 216-226.

18.   Palanisamy, K., and V. Subramanian, *CaCO3 scale deposition on copper metal surface; effect of morphology, size and area of contact under the influence of EDTA*. Powder Technology, 2016. **294**: p. 221-225.

19.   Söhnel, O., and J. Mullin, *Precipitation of calcium carbonate*. Journal of Crystal Growth, 1982. **60**(2): p. 239-250.

20.   Compton, R.G., and C.A. Brown, *The inhibition of calcite dissolution/precipitation: Mg2+ cations*. Journal of colloid and interface science, 1994. **165**(2): p. 445-449.

21.   Meldrum, F.C., and S.T. Hyde, *Morphological influence of magnesium and organic additives on the precipitation of calcite*. Journal of Crystal Growth, 2001. **231**(4): p. 544-558.

22.   Fernandez-Martinez, A., H. Lopez-Martinez, and D. Wang, *Structural characteristics and the occurrence of polyamorphism in amorphous calcium carbonate*, in *New Perspectives on Mineral Nucleation and Growth*. 2017, Springer. p. 77-92.

23.   Butt, H.-J., and M. Kappl, *Surface and interfacial forces*. 2018: John Wiley & Sons.

24.   Lédion, J., C. Braham, and F. Hui, *Anti-scaling properties of copper*. Journal of Water Supply: Research and Technology-Aqua, 2002. **51**(7): p. 389-398.